International Journal of Physics and Applications

E-ISSN: 2664-7583
P-ISSN: 2664-7575
Impact Factor (RJIF): 8.12
IJOS 2025; 7(2): 210-226

www.physicsjournal.in
Received: 12-08-2025
Accepted: 14-09-2025

Rekar Qadir Rahman
A) Bachelor's Degree in Science Physics at Salahaddin University, Erbil, Iraq
B) Master's Degree in Condensed Matter at Islamic Azad University, Tehran, Iran

Corresponding Author:
Rekar Qadir Rahman
A) Bachelor's Degree in Science Physics at Salahaddin University, Erbil, Iraq
B) Master's Degree in Condensed Matter at Islamic Azad University, Tehran, Iran

A review of gas sensors based on nanotubes and conducting polymers: Hybrid approaches

Rekar Qadir Rahman

DOI: https://doi.org/10.33545/26647575.2025.v7.i2c.195

Abstract
In the last decade, the possible development of hybrid gas sensors based on carbon nanotube (CNT), titanium nanotube (TiO_2 NT), and conducting polymer (e.g., polyaniline, PANI, and polypyrrole, PPy) makes them intriguing gaps to fill for temperature-sensitivity replacement on conventional metal oxide sensors at high temperature. They offer operation at room temperature, high sensitivity, and possible engineered selectivity. Focusing on multi-component architectures, this report first details the roles of materials and sensing mechanisms (chemiresistive, photocatalytic, polymer doping and heterojunctions), and then fabrication techniques (Arc, CVD, laser, hydrothermal) and their effects on microstructure and performance. Additionally, other important performance parameters such as sensitivity, limit of detection (LOD), response/recovery times, selectivity, stability and repeatability are presented including test procedures and uncertainty analysis. The final judgement is that ternary systems (for example CNT/PANI/TiO_2 or 2D/CNT/PANI) and CNT/PANI composites own a relatively more competitive sensitivity, selectivity and stability during the actual humid atmospheres. What the future holds is reducing the tests protocols, making the chalcogenides resistant to humidity and creating scalable manufacturing methods.

Keywords: Gas sensor, carbon nanotubes (CNTs), conducting polymers (PANI, PPy), TiO_2 nanotubes, hybrid structures, NO_2, NH_3, limit of detection (LOD), response time, selectivity

1. Introduction
Gas detection is one of the leading topics in industrial safety, environmental monitoring, medicine, and even in smart home systems [1]. Leaks or buildup of toxic gases such as ammonia (NH_3), nitrogen dioxide (NO_2), and carbon monoxide (CO) pose serious threats to human health as well as environmental sustainability. Conventional methods such as gas chromatography (GC) and mass spectrometry (MS), as accurate as they are, are time and cost-consuming as well as non-portable [2]. To this extent, the development of efficient, fast, and low-cost gas sensors, particularly on a nanoscale, has become increasingly important. During the last decades, metal oxide semiconductor (MOX) gas sensors such as ZnO, SnO_2, and TiO_2 have become of general interest due to their sensitivity and low prices [3]. Nevertheless, they work at elevated temperature (300-400 °C), and this results in high energy consumption and reduced lifetime [4]. Furthermore, their performance deteriorate dramatically in the presence of humidity resulting from water molecules adsorption, in which it poses a great barrier to applications. To get rid of these limitations, nanostructured materials especially carbon nanotubes (CNTs) and titanium dioxide nanotubes (TiO_2 NTs) have made them as promising candidates for gas sensors production [5]. The extreme surface-to-volume ratio, distinctive electronic properties, and multi-active sites for gas molecules adsorption facilitate the improvement of sensing performance in these one-dimensional nanostructures [6]. Moreover, CNTs have been reported to detect toxic gases like NH_3 and NO_2 at room temperature, as it has been verified from experiments [9]. One of the new routes taken to enhance the performance of CNTs even more is blending of CNTs with conductive polymers like polyaniline (PANI) [7]. They are used in order to expand sensitivity and selectivity with a minimal increase of response and recovery times. In particular, the PANI-CNT structures have shown very low limit of detections for NH_3 at stable ambient conditions. Such properties have made hybrid sensors one of the leading candidates for medical use e.g., in the diagnosis of kidney diseases using breath biomarker [8]. Due to the merits of photocatalysis and chemical stability as well as biocompatibility, Titanium dioxide nanotubes (TiO_2 NTs) also receive great attention in gas sensing research [9].

However, there are not too sensitive at room temperature and they also need appropriate surface modifications or doping by transition metals to allowing them work [10]. Now, TiO_2 NTs combined with CNTs and conducting polymers can also remain shortcomings of the single material to achieve better optimization of the sensor performance under environmental changes. However, the notable achievements concerning the design of nanotube-based gas sensors are shadowed by still-existing barriers such as long-term stability, multicomponent atmosphere sensitivity and up-scalability to industrial level [11]. Much has been conducted in controlled laboratory settings and less clear is the degree to which it performs in more realistic practice settings in sectors and clinical settings. More systematic study is also required for effects of humidity and cross-sensitivity by other gases [12].

Based on the existing literature, the integration of conducting polymer and carbon nanotubes along with titanium dioxide nanotubes has opened up new possibilities in the development of gas sensors. The present review article has been developed with an aim to critically analyze the sensing mechanism, synthesis procedures, and performance characteristics of hybrid sensors. The greatest novelty of this current study is the focus on multi-component and composite architectures approaches that can pave the way towards the development of a novel generation of stable, smart, and energy-efficient gas sensors for industrial, medical, and environmental applications.

2. Literature Review

In recent decades, the development of gas sensors has gained great importance due to their wide applications in environmental monitoring, industrial safety, and medicine. The first generation of these sensors was based on metal oxide semiconductors (such as SnO_2, ZnO, and TiO_2), which, despite their simplicity and low cost, required high operating temperatures and suffered from poor selectivity. Consequently, research attention shifted toward nanostructured materials capable of operating at room temperature. Among them, carbon nanotubes (CNTs) with high conductivity and large surface-to-volume ratio, conducting polymers (such as PANI and PPy) with doping capability and chemical stability, and titanium dioxide nanotubes (TiO_2 NTs) with photocatalytic properties played key roles. However, each of these materials alone had limitations, which led to the emergence of multi-component hybrid architectures. The integration of CNTs, polymers, TiO_2, and two-dimensional (2D) materials (such as MoS_2 and $MoSe_2$) created synergistic effects, resulting in significant improvements in sensitivity, selectivity, stability under humid conditions, and scalability. This evolution has defined the main trajectory of current research in gas sensors.

2.1 Metal Oxide Semiconductor (MOX)-Based Gas Sensors

Gas-sensing platforms were developed in the last decades as primary devices to be used in environmental monitoring, industrial safety and medicine. Initial sensors were developed on metal oxide semiconductors including SnO_2, ZnO and TiO_2 [13]. Their simplicity, low cost and reasonablly adequate sensitivity led to their widespread use. On the other hand, the required high working temperatures (300-400 °C) and low selectivity presented intrinsic challenges for their long-term utilization [14].

Various approaches have been used by researchers to enhance the performance of MOXs sensors by metal doping, surface modification [15]. Such implementations yield higher sensitivity, shorter response time, better short term stability, and higher surface reactivity. And the issue of high power losses at high operating temperatures remained unresolved. Also, thermal effects and gradual degradation of materials shorten sensor life and created a considerable limitation. In comparison to these issues, the intricacy of the manufacturing processes and the high cost of operations were additional factors that limited their use. This led to the emergence of a novel sustainable alternative of nanostructured materials that might be run at room temperatures [16].

2.2 Carbon Nanotubes (CNTs)

2.1. Metal Oxide Semiconductor (MOX)-Based Gas Sensors

Gas sensors emerged over the past decades as the simplest devices for applications in ambient air monitoring, personnel safety and health care. Most of the first sensors were developed using metal-oxide semiconductors like SnO_2, ZnO, and TiO_2 [13]. These were common due to their ease of use, low cost, and reasonable sensitivity. Their long-term application, nevertheless, was inherently impeded by the high working temperatures (300-400 °C) and low selectivity [14].

Several approaches like metal doping and surface modification were employed to enhance the performance of MOX sensor [15]. They allowed for the higher sensitivity and faster response time, short-term stability and surface reactivity. However, the issue of high power consumption at high working temperatures was not addressed. Additionally, sensor lifetime was limited and a critical barrier to success resulted from thermal phenomena and material progressive degradation. Their application was also further limited by the complexity of the processes required for manufacturing and the high cost of operations compared to these issues. Hence the trend toward nanostructured materials which would be useful at room temperatures evolved as an alternative, green solution [16].

Table 1: Remarkable Properties of Carbon Nanotubes (CNTs)

Comparison	Property Value	Property
Higher than carrier mobility in silicon	Room temperature: 79,000 $(cm^2)/(V's)$	Carrier mobility
1000 times greater than copper	Maximum current density > 10^9 A/cm^2	Maximum current density
Higher than diamond	Thermal conductivity: 6600 $W' m^{-1} K^{-1}$	Thermal conductivity
100 times stronger than steel	Tensile strength: 150 GPa	Tensile strength
Higher than diamond	Young's modulus: ~ 1 TPa	Young's modulus

Carbon nanotubes (CNTs) have been introduced as being among the most cutting-edge of materials within this family. With their high surface-to-volume ratio, high electron mobility, and capability of being coupled with other materials, CNTs have rapidly become one of the leading positions in gas sensor development [17]. They also show reasonable response to room temperature exposure of gases such as NH_3 and NO_2 [18]. Moreover, CNTs have unique one-dimensional structures, which provide the maximum number of channels for electron transport and thus the maximum response time. CNTs further

demonstrate this reliability by responding rapidly to abrupt variations in gas concentration, as established through experimental investigations.

The main benefit of CNT, apart from being functional at room temperature, is their ability to be modified and hybridized with various other materials. For instance, the addition of CNTs with precious metals or nanoparticles of oxides improved the sensor performance and selectivity [7]. Similarly, the hybridization of CNT with 2D nanostructure may give more active site of gas adsorption. However, clean CNTs are often ruin plagued by long-haul reliability, which warrants crossbreed methods and defensive coating [19]. It is particularly an issue for long-term industrial applications.

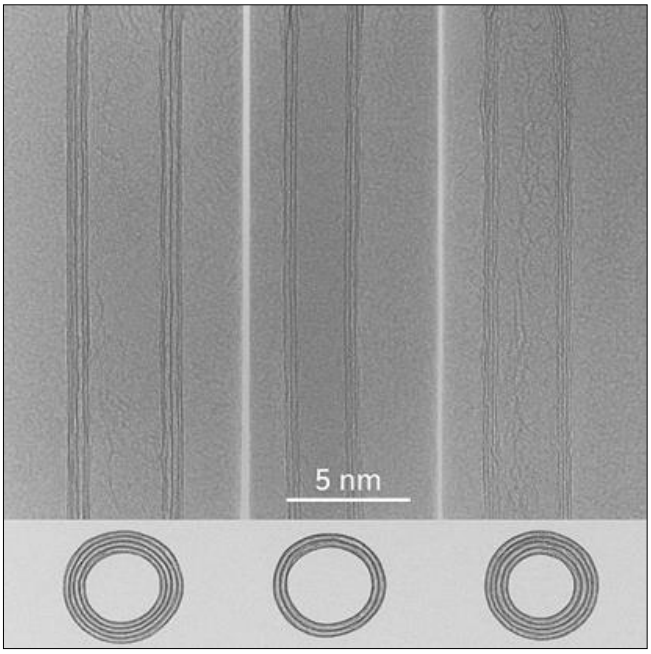

Fig 1: Transmission electron microscopy (TEM) image of multi-walled carbon nanotubes (MWNTs) discovered by Iijima.

The TEM image shown here was recorded by Iijima in 1991 and was recognized as the first experimental evidence for the existence of carbon nanotubes. At the bottom of each figure, cross-sections of the tubes are also displayed to reveal their multi-walled character. This tube-like structure is made up of many concentric layers of graphene rolled into coaxial tubes. The discovery of this structure was a major breakthrough in nanoscale science because the phenomenon of charge transport channels through multiple layers offered new conductive and mechanical opportunities.

Carbon nanotubes are classified into three types zigzag, armchair, and chiral based on the arrangement of their graphene sheets. The variation offers a variety of electrical and mechanical properties. Carbon nanotubes with chiral structures, for instance, can exhibit semiconducting properties.

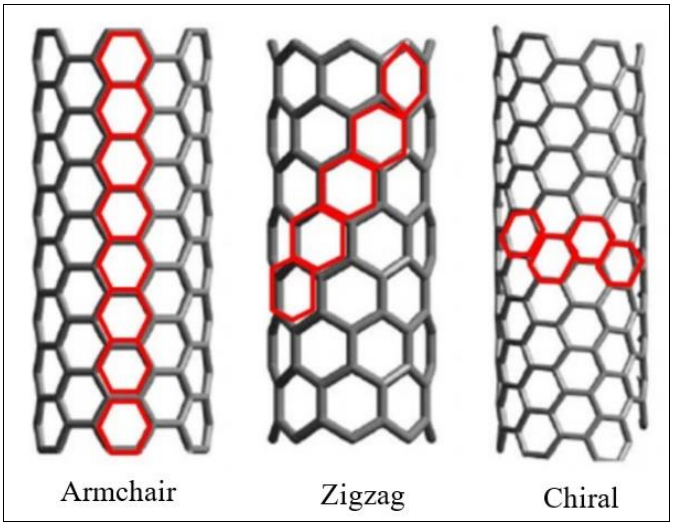

Fig 2: Types of carbon nanotube structures based on the chiral vector.

Chirality (the graphene lattice twist angle during tube formation) dictates the majority of carbon nanotube (CNT) electronic properties. Armchair CNTs are metallic, zigzag CNTs can be either metallic or semiconducting, and chiral CNTs are usually semiconducting. This characteristic forms the basis of selecting the nature of the CNT in devices such as nanoelectronics and gas sensors.

A carbon nanotube can be thought of as a rolled-up single graphene layer. Thus, the carbon atoms establish a hexagonal lattice structure. The hexagonal structure may be described in

terms of two lattice vectors:

$$a_1 = \left(\sqrt{3}/2\ a.\ a/2\right). \quad a_2 = \left(\sqrt{3}/2\ a.\ -a/2\right)$$

Where

$$a = |a_1| = |a_2| = 1.42 \times \sqrt{3} = 2.46\ \text{Å}$$

Here, a is the graphene lattice constant, which is derived from the C-C bond length in graphene (1.42 Å). These vectors span a two-dimensional Bravais lattice, as illustrated in Figure 1.

Schematic of the two-dimensional graphene Bravais lattice defined by vectors a_1 and a_2.

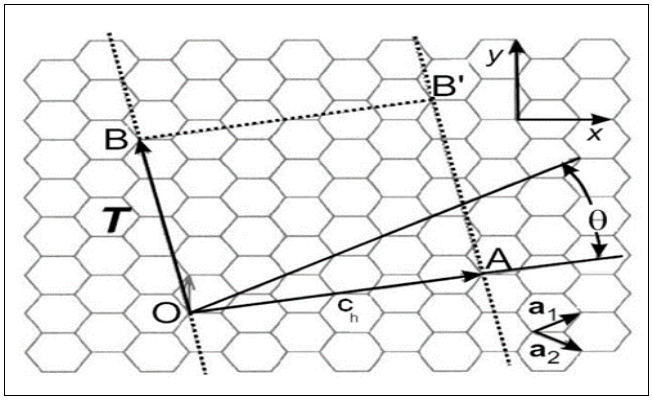

Fig 3: Hexagonal lattice representing a nanotube

Hexagonal lattice representing a nanotube. If point O is connected to A and B (or B'), the nanotube is described by the chiral vector $C_h = (4.2)$. This chiral vector defines a chiral rule, while the translation vector, which is perpendicular to the tube axis, is denoted by T_1 (adapted from).

This figure represents one of the infinite possible geometries of nanotubes. Nevertheless, all of them can be described with reference to the chiral vector:

$$C_h = na_1 + ma_2$$

Thus, nanotubes can be labeled by the integer pair $(n.m)$. Moreover, the chiral vector defines the circumference of the nanotube, while the nanotube axis is determined by the translation vector. The unit cell of a nanotube consists of the chiral vector and a translation vector parallel to the nanotube axis. The rectangular area defined by these two vectors represents the nanotube unit cell.

Therefore, the structural characteristics of a nanotube depend only on the two integers n and m. The vectors a_1 and a_2 are defined such that the angle between them is 60^∘. When there is a significant difference between the two vectors, special vectors arise, leading to specific types of nanotubes. Nanotubes with angular symmetry are referred to as zigzag or armchair. Their electronic properties are determined by the chiral angle. For example, the choice (n.0) corresponds to a zigzag nanotube, while (n.n) defines an armchair nanotube.

For a chiral angle of 30^∘, all nanotubes are metallic. Other nanotubes are characterized by chiral vector values between 0^∘ and 30^∘.

The fundamental structure of carbon nanotubes is based on a sheet of graphene rolled into cylindrical shape. Therefore, all the properties of carbon nanotubes are a function of the properties of the sheet of graphene. The resulting carbon nanotubes thus possess their own specific properties, which are regulated by the integers (n.m).

As indicated already, a nanotube can be visualized as a graphene sheet rolled up into a cylindrical tube with closed hemispherical caps. Due to the fact that they have the same lattice symmetries, the electronic band structure of carbon nanotubes can be seen as a translation of the graphene band structure, i.e., its dispersion bands.

In the graphene band structure at the K point, the valence band and conduction band intersect, attributed to the π and π^* orbitals. The π bands originate from the $2p_z$ orbitals of carbon atoms. Thus, the highest occupied state corresponds to the $2p_z$ orbital, in addition to hybridized combinations of $2s$, $2p_x$, and $2p_y$ orbitals, which result in the σ bands. Consequently, the conduction bands, chiral properties, and the energy characteristics of the band structures of carbon nanotubes can be interpreted solely through the planar π bands of graphene.

General schematic of metallic and semiconducting carbon nanotubes derived from graphene band structures.

Band Structure and Density of States of Carbon Nanotubes

$$E_{2D}(k_x.k_y) = \pm\gamma_0[1 + 4\cos(\sqrt{3}k_x a/2)\cos(k_y a/2) + 4\cos^2(k_y a/2)]^{1/2}$$

where γ_0 is the nearest-neighbor hopping integral. The valence and conduction bands intersect at six points, known as the K points. These points are determined by the chiral boundary conditions of the nanotubes when considering the cylindrical circumference, such that electrons are free to move only along the axial direction. This condition is related to the quantization of energy given by:

$$k_n C_h = 2\pi q. \quad q = 0.1.2. \ldots$$

The discrete allowed values of the wave vector k are represented as a set of equally spaced parallel lines in reciprocal space (Figure 1). The intersections of these lines with the two-dimensional energy bands indicate the allowed energy states in nanotubes. With respect to the chiral vector C_h and the translation vector T, the number of metallic or semiconducting bands with one-dimensional conduction channels along the nanotube axis can be identified.

According to this general formulation, as the nanotube diameter increases, the number of allowed energy lines also increases, leading to a larger unit cell size and a greater number of one-dimensional bands within the band gaps.

Schematic representation of the discrete allowed energy states of carbon nanotubes derived from the graphene band structure.

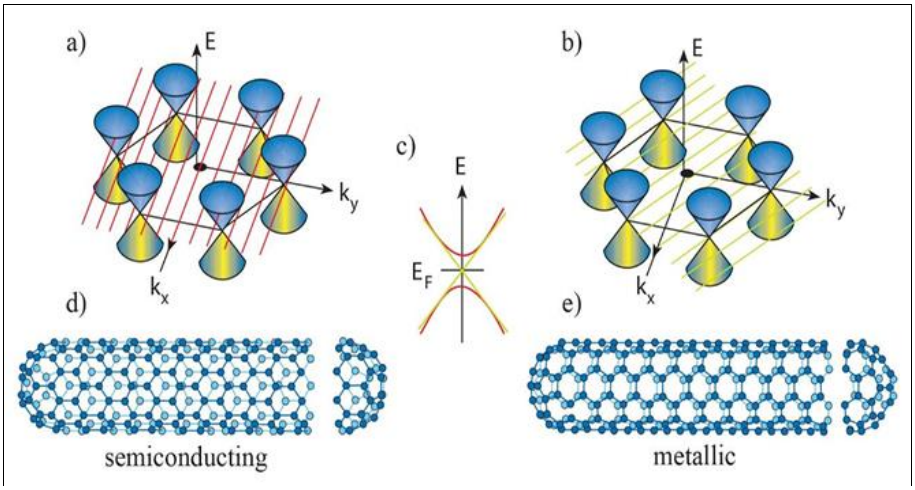

Fig 4: Band structure of metallic and semiconducting carbon nanotubes.

a) General diagram illustrating the band structure of a semiconducting nanotube.
b) General diagram illustrating the band structure of a metallic nanotube. The allowed electronic states are determined by the intersections of the allowed wave vectors (green-red lines) with the graphene band structure.
c) General diagram of the energy bands; metallic and semiconducting behavior. The first sub-bands are shown.
d) General diagram of the structure of a semiconducting zigzag nanotube.
e) General diagram of the structure of a metallic armchair nanotube. Adapted from [43].

The quantized energy wave vectors k, defined by the chiral vector, determine whether a carbon nanotube is metallic or semiconducting. If the allowed k-lines pass directly through one of the K points, the nanotube will be metallic. The electronic properties of carbon nanotubes (CNTs) are directly influenced by the chiral vector (n,m). This vector also determines whether a nanotube is metallic or semiconducting. In general, if (n,m) is a multiple of 3, the nanotubes become metallic; they are otherwise semiconducting. This unique dependence has helped make CNTs useful in a range of applications from nanoscale transistors to high-selectivity gas sensors.

To gain a better insight into this notion, looking at the density of states (DOS) of zigzag nanotubes having various (n,m) values can identify their electronic properties (Figure 5).

(a) Generic diagram of the band structure of a semiconducting nanotube. (b) Generic diagram of the band structure of a metallic nanotube. The allowed electronic states are characterized by the intersections of the allowed wave vectors (green-red lines) with the graphene band structure. (c) Generic diagram of the energy bands; metallic and semiconducting behavior. The first sub-bands are shown. (d) General structure diagram of a semiconducting zigzag nanotube. (e) General structure diagram of a metallic armchair nanotube. Adapted from.

The quantized wave vectors of energy k, which are given by the chiral vector, classify a carbon nanotube to be metallic or semiconducting. When the allowed k-lines pass directly through one of the K points, the nanotube will be metallic. The chiral vector (n,m) determines the electronic characteristics of carbon nanotubes (CNTs). The vector determines if a nanotube will be metallic or semiconducting. Generally, if (n-m) is a multiple of 3, the nanotubes will be metallic; otherwise, they are semiconducting.

This unique dependence has made CNTs suitable for a wide range of applications, ranging from nanoscale transistors to highly selective gas sensors. In order to obtain a deeper insight into this topic, investigation into the density of states (DOS) of zigzag nanotubes with different (n,m) values can reveal their electronic nature (Figure 2).

Density of states (DOS) of zigzag nanotubes for different (n,m) values, whether they are metallic or semiconducting.

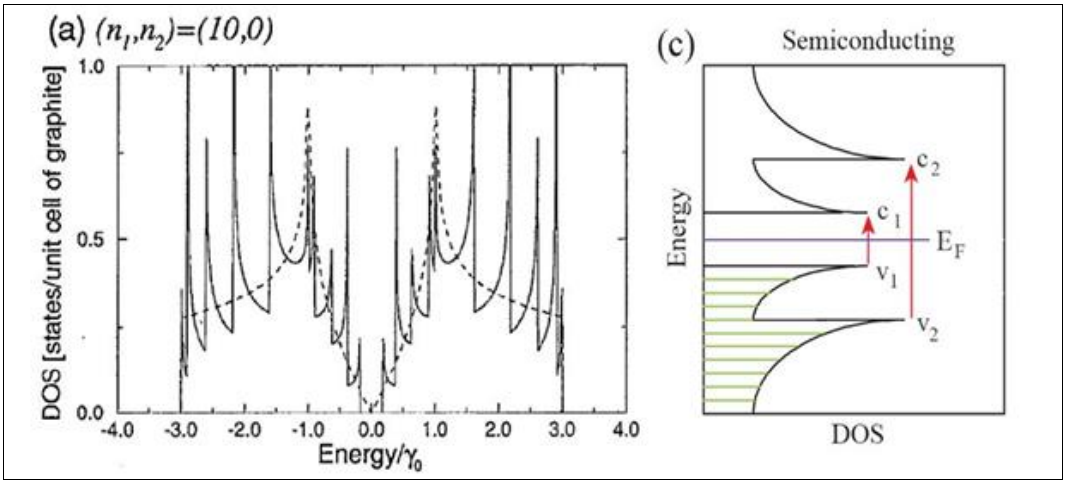

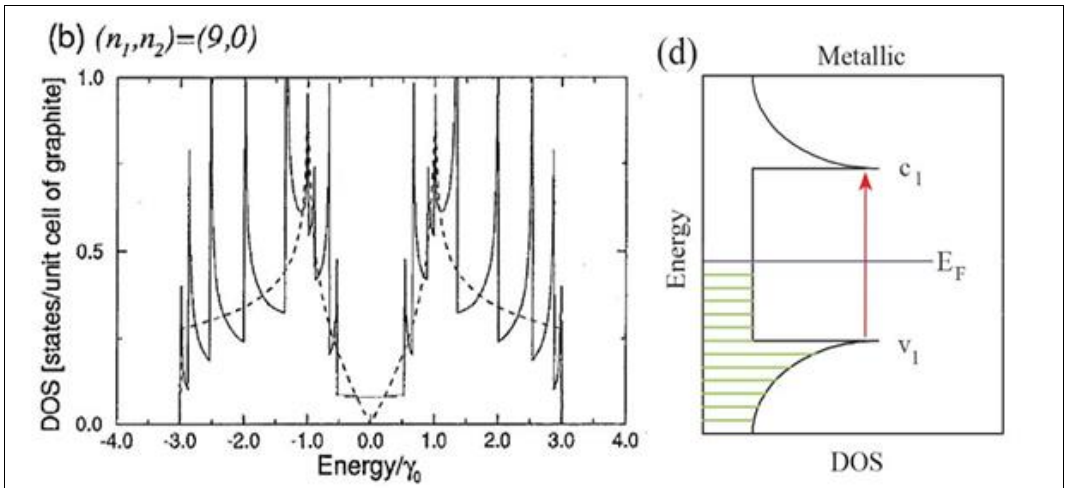

Fig 5: Comparison of the density of states (DOS) in semiconducting and metallic zigzag carbon nanotubes

The electronic density of states (DOS) of two various zigzag carbon nanotubes are plotted by Figure 1, which exhibit different properties based on their chiral vector (n,m).

For the case (0,10), as exhibited by Figures (a) and (c), there exists a big energy gap between the valence and conduction bands due to which the nanotube is semiconducting.In this case, Fermi level E_F is within the band gap, and electron transport has to be performed with excitation energy.

On the other hand, in the case of (0,9), as has been observed from Figures (b) and (d), the Fermi level crosses the energy bands directly and no gap is formed; thus, the nanotube is metallic.

This difference clearly indicates that a good difference in chirality parameters (n,m) can alter the electronic nature of CNTs from semiconducting to metallic. This unusual nature is the reason for their widespread use in nanoscale electronics and sensing.

Comparison of electronic density of states (DOS) for semiconducting ((0,10)) and metallic ((0.9)) zigzag carbon nanotubes.

2.3 Conducting Polymers

Conducting polymers such as polyaniline (PANI) and polypyrrole (PPy) have also been suggested as alternative materials for CNTs owing to their ease of processing, chemical stability, and conductivity [20]. PANI/CNT hybrid architectures have been shown to have considerably improved sensitivity and decreased detection limits compared to their respective individual counterparts in recent publications [21]. In addition, such architectures have the ability to reduce sensor recovery times by a huge amount, and these are therefore useful for the detection of toxic gases in real-time and rapid applications.

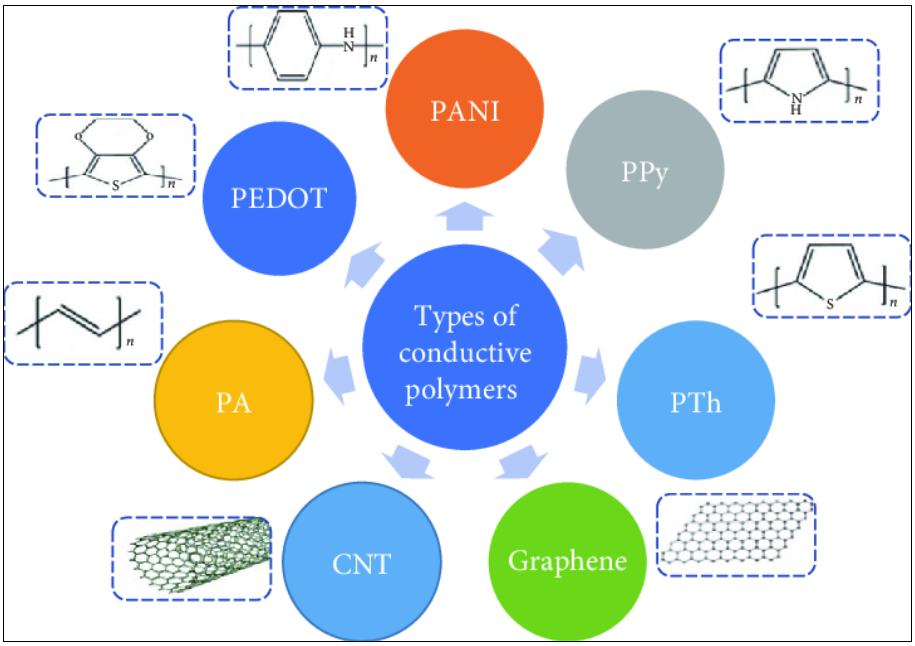

Fig 6: Types of conducting polymers and composite nanostructures used in sensors.

The different classes of conductive polymers like polyaniline (PANI), polypyrrole (PPy), polythiophene (PTh), polyacetylene (PA), and poly(3,4-ethylenedioxythiophene) (PEDOT) and carbon nanostructures like carbon nanotubes (CNTs) and graphene are depicted in Figure 6. According to the performance in terms of conductivity, chemical stability, tunability of structures, though, all the materials mentioned above are the essential building blocks for the construction of high-performance gas sensors.

The synergistic effects obtained by the combination of these conducting polymers with nanostructures like CNTs and graphene contribute to their increase not only in selectivity

and sensitivity but also the sensors' environmental stability. Structures of this type are a promising avenue toward the new family of high-performance sensors that can be used for industrial, medical and environmental monitoring applications

2.4 Titanium Dioxide Nanotubes (TiO_2 NTs)

In addition to conducting polymers and CNTs, titanium dioxide nanotubes (TiO_2 NTs) have also been of interest. Due to their photocatalytic and biocompatibility, such nanomaterials were employed in gas sensing of various gases [22]. Pure TiO_2 NTs possess relatively low conductivity, however, and thus are required to be doped or functionalized with other materials to make them more effective [23].

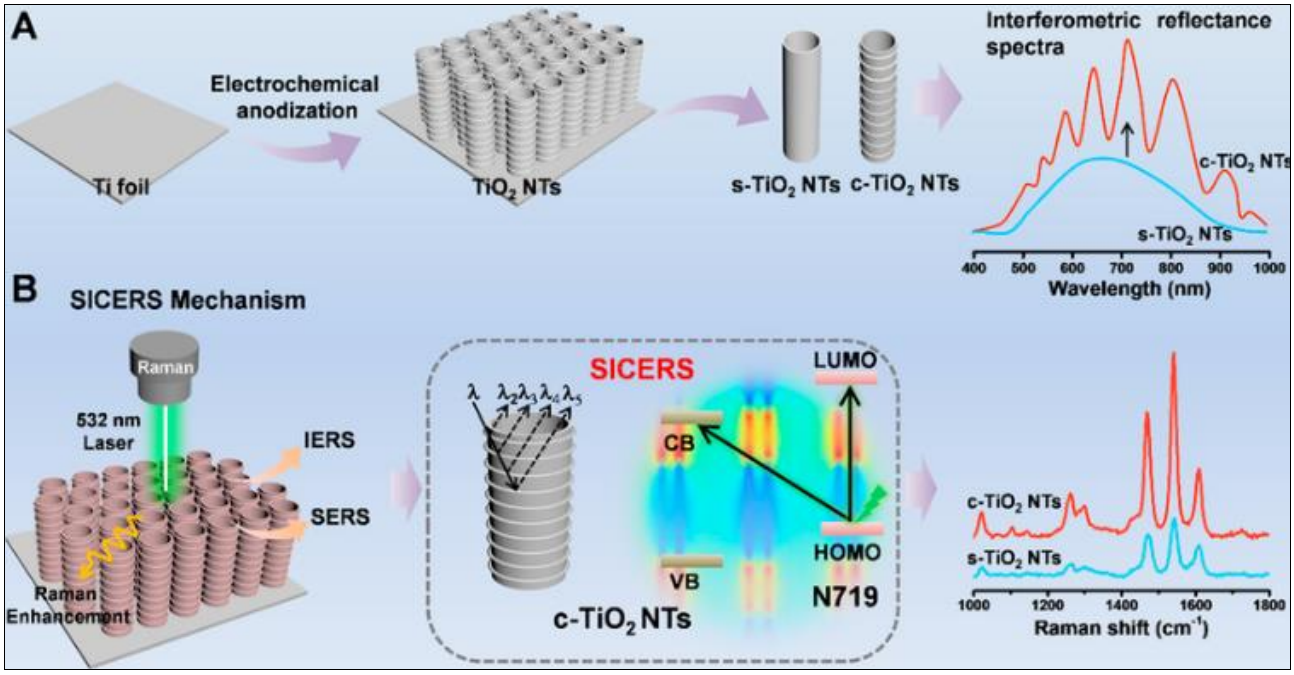

Fig 7: Synthesis process of titanium dioxide nanotubes (TiO_2 NTs) via electrochemical anodization and the SICERS mechanism for Raman signal enhancement.

The synthesis mechanism and working process of titanium dioxide nanotubes (TiO_2 NTs) and the functionalized architecture are illustrated in Figure 7. Figure part (A) illustrates the process of electrochemical anodization to synthesize the TiO_2 NTs from a titanium sheet for the production of two types of nanotubes, i.e., amorphous (s-TiO_2 NTs) and crystalline (c-TiO_2 NTs). The interference reflection spectrum indicates that the crystalline sample contains more absorption and optical response.

In part (B), the (SICERS) process is introduced, where green laser excitation (532 nm) of TiO_2 NTs enhances the Raman signal due to SERS and IERS effects. The figures show that c-TiO_2 NTs, owing to their crystal structure, offer greater signal intensity and sensitivity compared to s-TiO_2 NTs. The results highlight the importance of optimizing the structure of TiO_2 NTs for improving performance in sensing and photocatalyst applications.

2.5 Multi-Component Hybrid Structures: In recent years, multi-component hybrid composites such as $MoSe_2$/PANI/Ti_3C_2Tx have been introduced, which can simultaneously provide high sensitivity, good selectivity, and long-term stability [24]. These structures, in particular, have shown superior performance under high-humidity conditions, opening new horizons for gas sensor design [25]. One of the major challenges in the field of gas sensors is the effect of humidity and the presence of interfering gases. Water molecules can occupy active surface sites, thereby reducing the sensor response. Recent studies have demonstrated that the use of two-dimensional (2D) materials such as MoS_2 and $MoSe_2$, in combination with CNTs or PANI, can mitigate the effects of humidity [26].

Another challenge is industrial scalability. Many studies have been conducted at the laboratory scale, and the transition of these technologies to industrial scale faces difficulties such as layer uniformity and high production costs [27]. In this regard, electronic printing methods and novel nanostructuring technologies have been introduced as promising solutions [28].

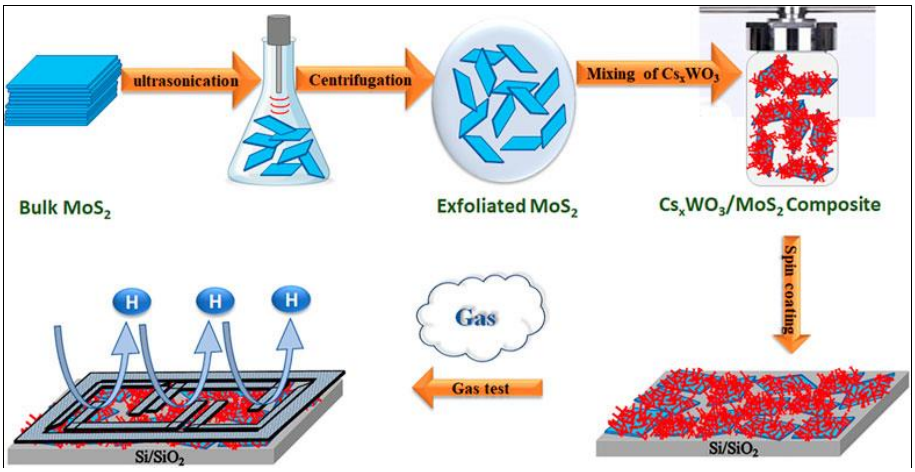

Fig 8: Synthesis process of titanium dioxide nanotubes (TiO_2 NTs) via electrochemical anodization and the SICERS mechanism for Raman signal enhancement.

Hybrid approaches combining MoS_2 and Cs_xWO_3 for gas sensing are illustrated in Figure 8. On the left, the exfoliation process of MoS_2 into thin, two-dimensional sheets is shown. These sheets are then integrated with Cs_xWO_3 to form the final nanocomposite with sensing capabilities. Correct, once they have been deposited onto a substrate, the sensor is constructed and sensing performance in gas detection determined. This is an illustration of a multi-component hybrid design, demonstrating how 2D materials (such as $MoSe_2$ or MoS_2) may be combined with other components to deliver better sensing performance and humidity stability.

Such multi-component hybrid composites are in fact a fresh approach for overstepping the typical gas sensor constraints. By exploiting the synergistic benefits of their functionalities, such as the enhanced active surface area of 2D (MoS_2/$MoSe_2$), the conductivity of carbon nanotubes (CNTs) and stability of the conductive polymer (PANI), they provide a highly multi-functional platform for improving sensor metrics. In addition to higher sensitivity and selectivity, these architectures allow for improved stability during operation under various environmental conditions and at elevated humidity levels. Thus, new class of smart materials, hybrid composites may open a new avenue for sensors with a wide range of potential applications from health to environmental monitoring.

The blinding flash of progress has occurred, but a few core issues continue to be front and center. The overcoming challenges of scalable and uniform fabrication at the industrial scale, quality assurance and low-cost manufacturing of these structures. Novel techniques like electronic printing, nanostructure self-assembly methods, and layer-by-layer coating technology have great potential to provide practical solutions for these issues. Future research in this field is focusing on emerging technologies and multi-component hybrid composites with more intelligent designs, so that gas sensors can be not only potentially realized under laboratory conditions but also performed stable and cost-effective in actual industrial and medical environments.

3. Sensing Mechanisms

The sensing mechanisms in hybrid nanostructures based on nanotubes and conducting polymers are primarily governed by changes in the electrical properties of the materials when interacting with gas molecules. This section examines the fundamental principles and the role of different components in enhancing sensor performance.

- **Chemiresistive Mechanism**
  The change in the electrical resistance of the sensing material is caused by the gas molecule reaction or adsorption onto its surface. For instance, for the composites such as CNTs or TiO_2 nanotubes, target gas adsorption (e.g., NO_2 or NH_3) causes charge transfer (electrons or holes) between the gas molecules and the material surface. When the gas is an oxidizing gas, electrons are stripped away from the sensor, and the resistance rises; when the gas is a reducing gas, electrons are added to the sensor, and the resistance falls (Figure 9).

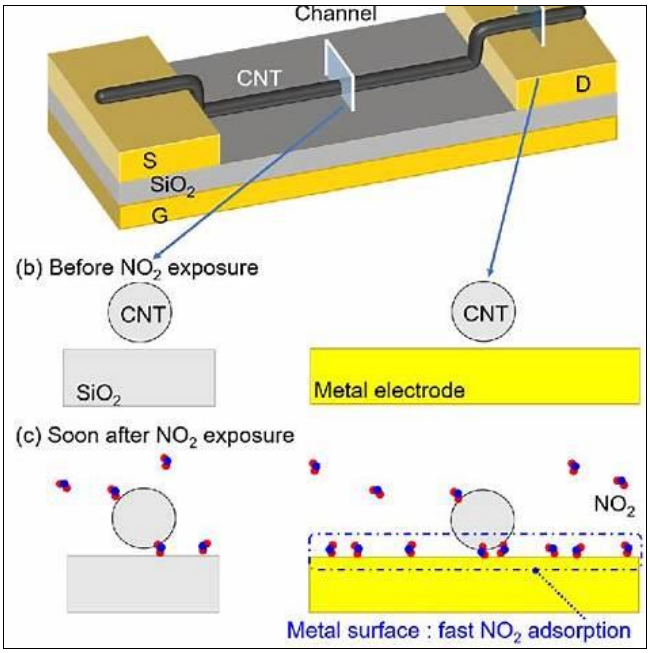

Fig 9: Chemiresistive mechanism in a CNT-based sensor; change in resistance before and after adsorption of NO_2 gas [29].

The schematic above illustrates a CNT-based sensor: the left side shows the state before exposure to the gas, while the right side shows the state after gas adsorption—where gas molecules interact with the CNT surface and the electrical current between the electrodes is affected [29].

In titanium dioxide nanotubes (TiO_2 NTs), this mechanism is further enhanced due to the presence of inner tube surfaces and inter-tube boundaries. Gas adsorption on the inner and outer surfaces of the tubes induces changes in charge

distribution and in the width of the depletion layer; these changes in the depletion layer lead to variations in the overall conductivity of the TiO_2 structure, ultimately resulting in a measurable signal. Moreover, in hybrid structures where TiO_2 NTs are combined with CNTs or conducting polymers, charge transport pathways are improved and the resistance change becomes more directional, thereby increasing both sensitivity and response speed.

- **Photocatalytic Mechanism**
  In photocatalysis particularly in titanium dioxide nanotubes (TiO_2 NTs) electrons are excited from the valence band (VB) to the conduction band (CB) by UV or visible light photon absorption, generating electron-hole pairs (e^-/h^+). Under light irradiation, holes (h^+) can oxidize hydroxyl groups or water molecules to generate reactive radicals such as •OH, while electrons in the conduction band can reduce oxygen molecules to superoxide anions (O_2^-•). In aggregate, these responses lead to the breakdown of chemical gases or adsorption and modification of electrical sensor surface properties.
  In TiO_2 NTs, due to their tubular structure, the high surface-to-volume ratio enables inner as well as outer tube surfaces to participate in light absorption and reaction, hence increasing photocatalytic activity. During hybridization of TiO_2 NTs with other materials two-dimensional materials or nanocarbons the charge carriers, electrons, and holes are being separated, and recombination is being inhibited. This leads to enhanced photocatalytic activity under visible light, increased sensor sensitivity, and enhanced performance under realistic environmental conditions, particularly with humidity and natural light present.
  The main photocatalytic process in semiconductors such as TiO_2 is shown in Figure 10 [30].

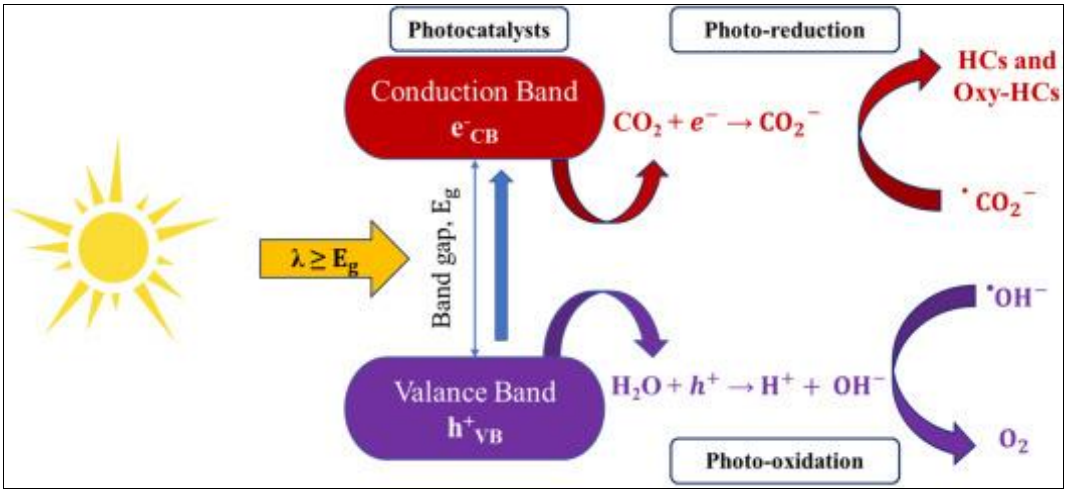

Fig 10: Schematic of the photocatalytic mechanism in semiconductors under light irradiation [30].

Upon photon absorption with energy equal to or greater than the band gap (Eg_gg), electrons are excited from the valence band (VB) to the conduction band (CB), forming electron-hole pairs (e^-/h^+). The photo-excited electrons in the CB also facilitate reduction reactions (photo-reduction), the products of which are superoxide ions (•O_2^-), able to degrade hydrocarbons and hydrocarbon derivatives. In the meantime, other holes (h^+) in VB initiate oxidation reactions (photo-oxidation), where oxidation of hydroxyl ions or water molecules creates hydroxyl radicals (•OH) which are the initiators for breaking organic molecules and toxic gases. In combination, such mechanisms are the reason for high efficiency of gas sensors and removal of polluting gases in TiO_2 and other semiconductors.

- **Conducting Polymers' Role in the Sensing Mechanism**
  Polyaniline (PANI) and polypyrrole (PPy) are among the most important conducting polymers used in gas sensors. Due to their conjugated π-bonded chain systems as well as doping capacity, they are very electrically conductive. The natural state of these polymers is a semiconductor state and need to be doped for their effective sensing performance PANI usually through protonation and PPy through chemical or electrochemical oxidation.
  Doping inserts a charge carrier with positive charge (bipolaron or polaron) within the polymer chains, and counter-ions (e.g., anions) become localized in the vicinity of the chains to maintain charge neutrality. Upon contact of the surface of a conducting polymer with oxidizing gases, such as nitrogen dioxide (NO_2) or reducing gases, such as ammonia (NH_3), the doping concentration or the state of the charge carrier is altered. For example, an oxidising gas would strip electrons from the polymer backbone, thus increasing the concentration of polarons or bipolarons and thus the conductivity whereas a reducing gas induces the reverse redox effect, thus lowering conductivity. Such conductivity variation offers quicker response and lower detection limits [31].
  One of the biggest challenges in the application of these polymers is sustaining stable performance under environmental conditions, especially when exposed to air and moisture. Water may interfere by reacting with the sites of doping or the surface of the polymer, thus influencing conductivity. To prevent these inputs, hybrid systems particularly PANI or PPy and CNTs, TiO_2 NTs, and two-dimensional materials like $MoSe_2$ have proven beneficial. These hybrid systems, in addition to promoting enhanced charge transport pathways and electron-hole separation, also protect active sites, resulting in stable sensor response under real environmental conditions (i.e., varying temperature and humidity).
  The figure above is a schematic diagram of a conducting polymer film on a semiconducting or metallic substrate, showing charge carriers and the effect of gas interaction on the surface. Such representations enable the reader to

better visualize the process of conductivity change and the doping role in the sensor mechanism of polymers.

- **Hybrid Mechanisms**
  Hybrid mechanisms are primarily based on synergistic effects among different components e.g., carbon nanotubes (CNTs), titanium dioxide nanotubes (TiO_2 NTs), and conducting polymers. Each component contributes its specific advantage: CNTs provide high electronic conductivity and fast charge transport paths; TiO_2 NTs provide a high active surface area, chemical stability, and photocatalystic activity; and polymers provide doping ability and fast response to oxidizing or reducing gases.
  When blended in a hybrid construction, all these advantages can be utilized at once.
  For example, CNT/PANI/TiO_2 NT composites are structures that can deliver high baseline electrical conductivity, activate the photocatalytic function of TiO_2 under illumination or applied voltage, and offer a polymer surface sensitive to gases thereby producing distinct changes in resistance or current.
  In such structures, doping and charge separation occur in a more systematic manner. CNTs typically serve as efficient carriers of electrons or holes, TiO_2 provides surfaces where oxygen or gas molecules can be adsorbed, and polymers (such as PANI or PPy) act as interfacial layers or sensitive coatings. Moreover, the formation of heterojunctions between TiO_2 and CNTs, or between TiO_2 and polymers, leads to the creation of depletion layers that are more responsive to variations in gas concentration. As illustrated in Figure 10, these hybrid configurations enhance the energy difference between the conduction band and the interfacial states, thereby amplifying the electrical response to gas concentration changes [32].

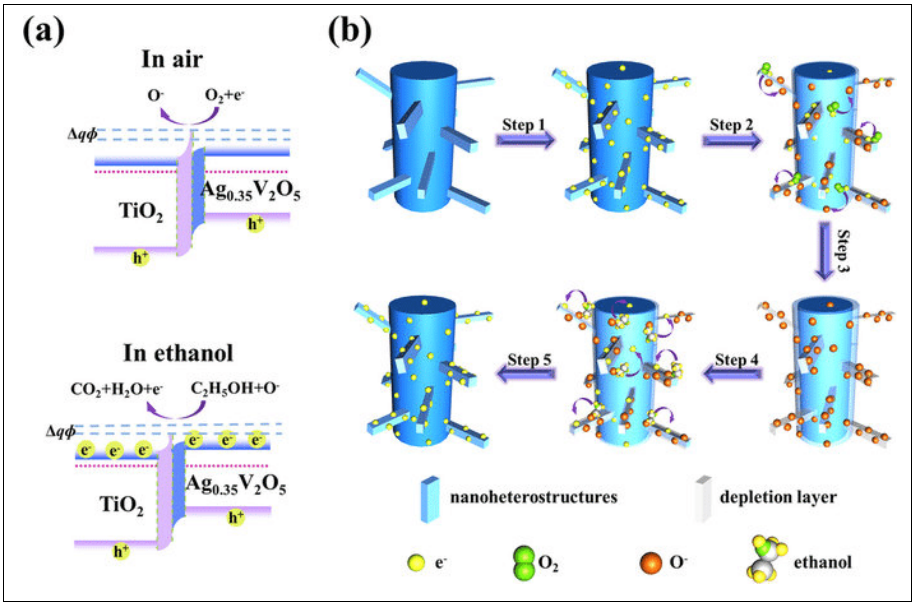

Fig 11: Gas sensing mechanism in branched $TiO_2/Ag_{0.35}V_2O_5$ nanoheterostructures under exposure to air and ethanol vapor [33].

In Figure 11, the gas sensing mechanism in branched $TiO_2/Ag_{0.35}V_2O_5$ nano heterostructures is illustrated. In part (a), the band structure model is shown under air and ethanol conditions. With air, oxygen is adsorbed onto the surface, trapping electrons and forming a depletion layer, but in the presence of ethanol, redox reactions (conversion of O^- to CO_2 and H_2O) release electrons and reduce the energy barrier.
In part (b), the sensing mechanism step by step is shown: starting from the initial adsorption of oxygen (steps 1 and 2), followed by the formation of the depletion layer (step 3), then the reaction between ethanol and the adsorbed oxygen species (step 4), and the release of electrons and the increase in conductivity (step 5). This cycle confirms that the coupling of TiO_2 with $Ag_{0.35}V_2O_5$ can enhance the responsiveness and sensitivity of the sensor in ethanol vapor detection significantly.

4. Methods of Synthesis/Fabrication and Hybrid Architectures

4.1. Synthesis of Carbon Nanotubes

Carbon nanotubes (CNTs), one of the most important carbon nanostructures, have been widely applied in sensing, energy, and nanoelectronics due to their outstanding mechanical, electrical, and thermal properties. A variety of techniques have been developed for CNT synthesis, each with some advantages and limitations. The choice of technique depends on the required quality, cost, product purity, and amount to be synthesized.

- **Arc Discharge Method**
  The arc discharge technique is one of the earliest techniques used for CNT synthesis, where an electric discharge is carried out in an inert atmosphere between two electrodes. The technique generates temperatures of 4000-6000 K, with which high-quality CNTs can be synthesized. Single-walled CNTs (SWCNTs) can be produced using pulsed arcs, while other conditions tend to generate multi-walled CNTs (MWCNTs). Product quality depends on variables including current, voltage, plasma temperature, and electrode size. Although this process produces pure and stable CNTs, it is not preferred for large-scale industrial use due to its scalability challenges (Figure 12).

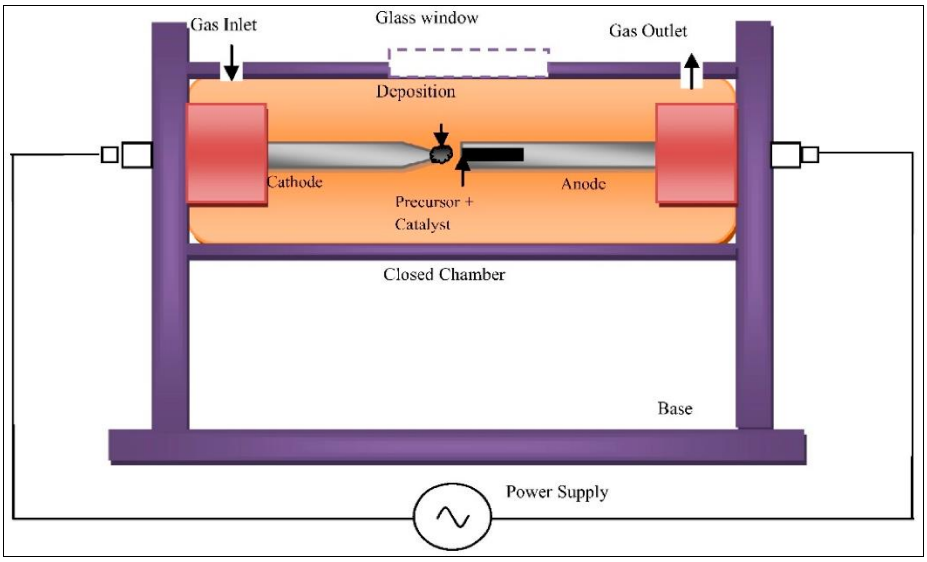

Fig 12: Schematic illustration of the arc discharge process and the formation of carbon nanotubes (CNTs). Reproduced with permission [34].

Figure 12 is a schematic diagram of the equipment employed for the preparation of carbon nanotubes (CNTs) by the arc discharge method. A closed vessel maintained in an inert atmosphere is constructed in which two graphite electrodes (anode and cathode) are placed. A source of power creates a high electric current, and by the creation of an electrical discharge between the two electrodes, highly hot temperatures between 4000-6000 K are generated. At these temperatures, the carbon precursor as well as the catalyst vaporize and get deposited on the cathode, and therefore CNTs are formed. The entry of inert gas from one end of the chamber and its exit from another provides a stable environment for the arc discharge and growth of CNTs. This is credited to be one of the oldest and most used techniques for the production of high-quality CNTs, although its industrial potential is still limited.

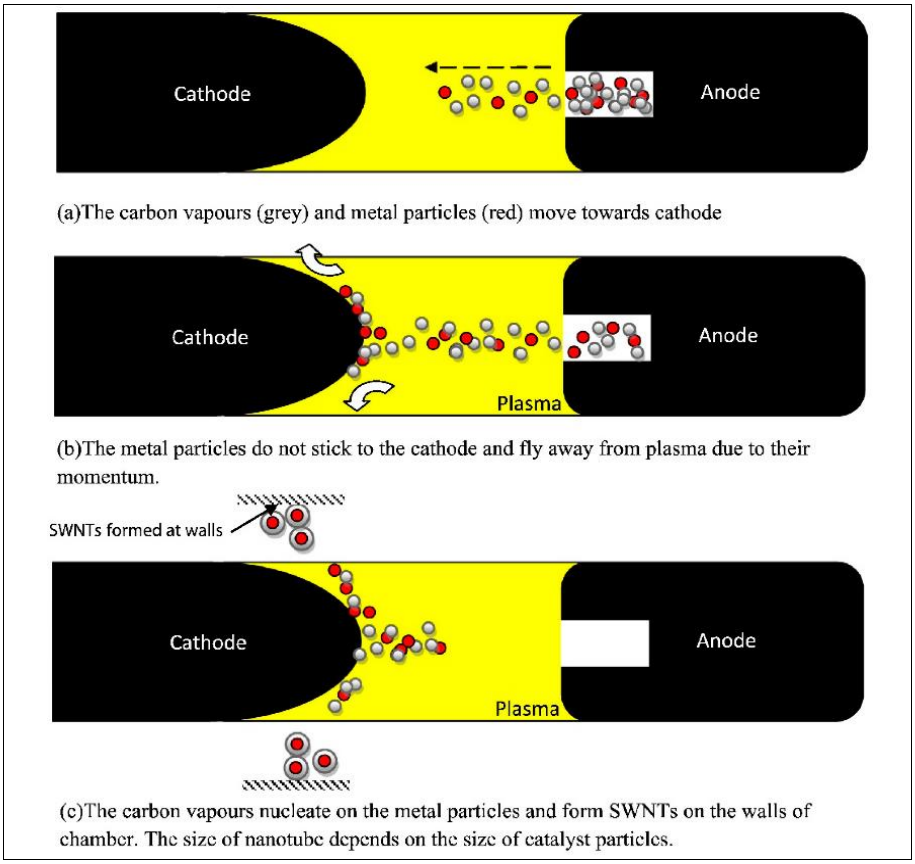

Fig 13: Graphical illustration of the catalyst's role in synthesizing carbon nanotubes (CNTs) using the arc discharge method. Reproduced with permission [34].

Figure 13 illustrates the function of the catalyst during single-walled carbon nanotube (SWCNT) synthesis in the arc discharge method. Metallic catalyst particles (red dots) and carbon vapors (gray dots) move from the anode to the cathode. In part (b), the metallic particles, due to their large momentum, do not get deposited on the cathode and remain dispersed in the plasma. In part (c), carbon vapors condense and nucleate on the metallic particles and lead to the growth of single-walled carbon nanotubes on chamber walls. The diameter of the grown nanotubes will be a function of the

catalyst particle size. This verifies that, in addition to arc discharge parameters (plasma power, arc current, and electrode geometry), the composition and size of the catalyst are also crucial in establishing the yield and quality of CNTs.

- **Chemical Vapor Deposition (CVD) Method**
  The least expensive and most widespread technique for mass production of CNTs is the CVD process. Hydrocarbon gases such as methane or acetylene are broken down in the presence of metal catalysts (Ni, Co, or Fe) at 600 to 900 °C, and the released carbon atoms are precipitated on the catalyst surface. This technique allows for good control of CNT type, length, and diameter (single-walled or multi-walled). One can also improve the structure and quality of CNTs through the optimization of reaction conditions and catalyst type.The greatest advantage of CVD lies in the possibility of performing mass production at low cost with the facility to design the process easily, for which reason it is the industry's favored method to produce CNTs [35].

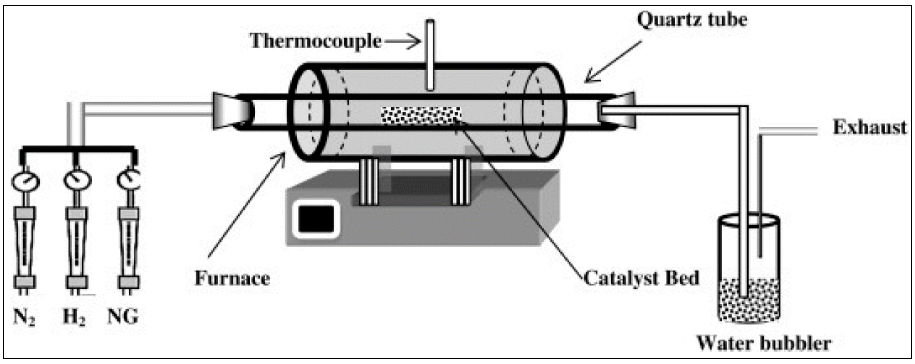

Fig 14: Typical schematic of the catalytic chemical vapor deposition (CCVD) process for synthesizing carbon nanotubes (CNTs) using methane. Reproduced with permission [35].

Figure 14 is a schematic illustration of CCVD apparatus for CNT synthesis. In this process, a quartz tube serves as the reactor where inside it the catalyst substrate is placed. Carrier gases (e.g., N_2 or H_2) and carbon source (e.g., methane or natural gas) are introduced into the reactor and thermally decomposed at high temperature (500-1200 °C). With the presence of metallic catalysts (e.g., Ni, Co, or Mo), carbon atoms are precipitated and carbon nanotubes form on the surface of the catalytic substrate. Reaction conditions and temperature are regulated with a thermocouple and observed, and exhaust gases are vented outside after passing through a water bubbler.

The main advantage of CCVD over methods such as arc discharge or laser ablation is the fine control of the diameter, length, and even the morphology of the nanotubes (single-walled or multi-walled). Moreover, it is scalable in an industrial setting and to mass produce CNTs at lower cost and higher purity. The form and size of the particles of the catalyst also play a crucial role in determining what dictates the growth mechanism: tip-growth is generally what occurs with big particles, whereas base-growth is the favored mechanism for small particles. Manipulation of the chemical and physical conditions of the catalyst is therefore the best way to yield high-quality CNTs of a desired size.

- **Laser Ablation Technique and Other Techniques**
  This method can yield pure and high-quality single-walled carbon nanotubes (SWCNTs). SWCNTs were grown by Zhang *et al.* [36] using bimetallic catalysts (NiCo and NiFe) and through the laser ablation method at 1200 °C for one hour. The information demonstrated that the diameter of the synthesized nanotubes grew when the content of iron (Fe) was improved; however, Raman spectroscopy showed that the yield of SWCNT did not alter with a focus on increment up to 0.5% iron concentration.

In another study, Zhang *et al.* [37] employed a continuous-wave CO_2 laser ablation technique with laser power ranging from 500 to 850 W to produce SWCNTs. The production yield was estimated at about 70%, and the diameters of the SWCNT bundles ranged from 6 to 20 nm. Analysis of the intensity of Raman radial breathing mode peaks confirmed the successful synthesis of SWCNTs, although the yield varied depending on the laser power.

Buta *et al.* [38] reported a mouse-shaped laser ablation chamber designed for the production of SWCNTs with minimal metallic catalyst. Transmission electron microscopy (TEM) and high-resolution transmission electron microscopy (HRTEM) confirmed the formation of 1.4 nm diameter nanotubes, encased in amorphous carbon. The formation of amorphous carbon along with SWCNTs on the surface of Pt-Co catalysts is observed in figure 15. The sizes of isolated nanotubes were found to range 1.2-1.5 nm in diameter with the greatest purity of SWCNTs achieved with 0.6 atomic% Co + 0.6 atomic% Ni. Lastly, it was suggested that the use of a longer quartz tube will increase the SWCNT production up to 70%.

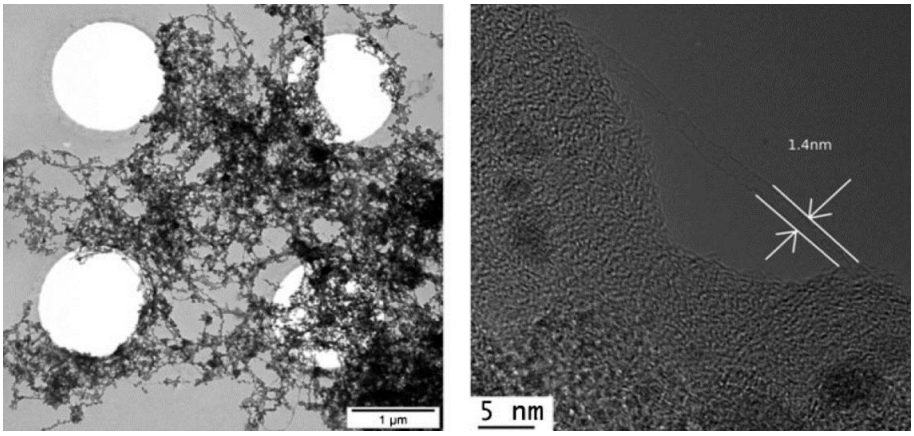

Fig 15: TEM and HRTEM images of the products obtained from laser ablation, showing a network of single-walled carbon nanotube (SWCNT) bundles and amorphous carbon. Reproduced with permission [38].

Yuge *et al*. [39] used the continuous wave (CW) CO_2 laser method at room temperature to yield crystalline multi-walled carbon nanotubes (MWCNTs) at a higher yield. Similarly, Hameed *et al*. [40] prepared graphene sheets and carbon nanostructures with pore diameters of 7 to 16 nm. This was accomplished by changing the laser energy in the laser ablation of carbon target in a liquid phase. Abstract The experimental results show that the pulsed laser ablation (PLA) was better purity and the maximum yield of single-walled carbon nanotubes (SWCNTs). The nanotubes appeared as entangled helical bundles that were a few hundred micrometers long. In addition, it was observed that max yield of SWCNT production was recorded at higher laser intensity and increased temperature of the furnace.

Tabatabaie and Dorranian [41] A pulsed laser vaporization method for carbon nanostructures and graphene nanosheets from graphite in liquid nitrogen. A high yield of graphene nanosheets was achieved at lower laser intensities but carbon nanoparticles and fluorine-containing species were formed at the higher laser intensities greater than 1.1 J/cm².

On the other hand, Mafi and Mostafa [42] reported that a SnO_2/MWCNT nanocomposite can serve as an efficient adsorbent for the removal of copper ions (Cu^{2+}) from wastewater. As can be seen from Figure 16, this nanocomposite was synthesized using pulsed laser ablation and had high adsorption capacity at pH 5.7The experiments further showed that the adsorption capacity increased with concentration of copper ions and finally attained equilibrium when the surface of the adsorbent was saturated.

The parameters of the laser used were wavelength 1064 nm, pulse duration 7 ns, and repetition rate 10 Hz. The suspension of the SnO_2/MWCNT nanocomposite was poured into a plastic filter chamber after synthesis and then heat-treated at 300 °C for 2 hours in a nitrogen atmosphere.

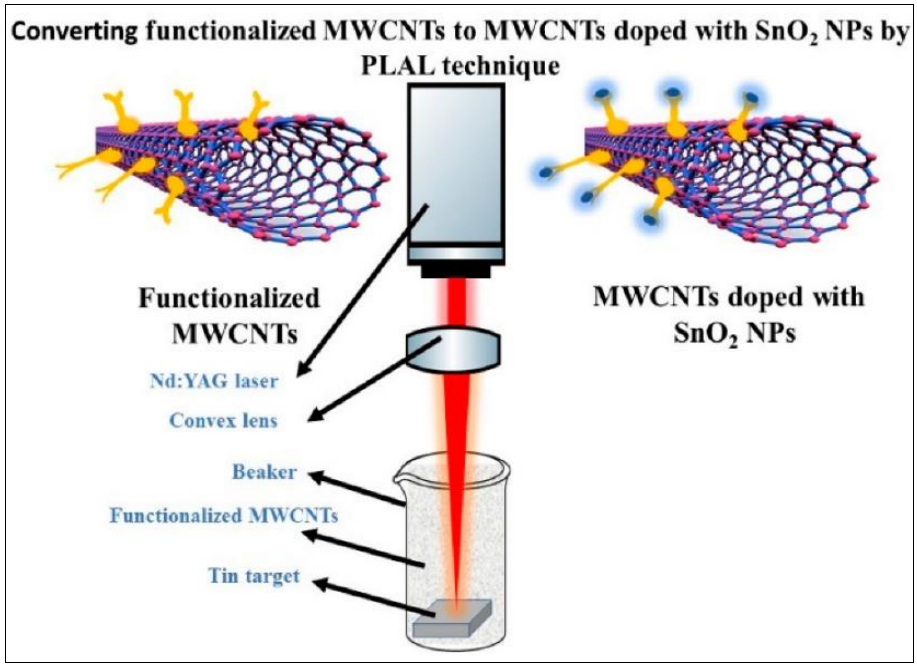

Fig 16: Preparation of SnO_2/MWCNT nanocomposites. Reproduced with permission [42].

Other synthesis processes of CNTs have also been reported. Sonochemical/hydrothermal process is used for the fabrication of structures such as carbon nano-onions, nanorods, and multi-walled carbon nanotubes (MWCNTs) having a few up to more than 100 layers of carbon. Hydrothermal synthesis is used to prepare nanotubes of diameter of about 60 nm, length 2-5 μm, and inner pore diameter 10 to 80 nm.

The electrolysis method is based on the electrochemical precipitation of alkaline earth metals onto a graphite cathode within molten NaCl at 810 °C under an inert argon atmosphere. MWCNTs formed by this method usually have

diameters between 10 and 20 nm and lengths of about 500 nm, formed by the cathodic reduction of CO_2 into elemental carbon on metal electrodes.

Finally, the solar method has been employed for the gram-scale synthesis of single-walled carbon nanotubes (SWCNTs). In this approach, a 50-kilowatt solar reactor with a Ni-Co catalyst is used. The quality of the resulting product is highly dependent on the evaporation temperature, which remains in the range of 2627-2727 °C [42].

5. Performance Metrics and Evaluation Protocols

For evaluating hybrid sensors based on CNTs, PANI, and TiO_2 NTs, standard metrics such as relative change in resistance or current, normalized sensitivity, limit of detection (LOD), and linear range are typically reported. Response time and recovery time also indicate the ability of the sensor to perform real-time monitoring and should be provided under specified temperature and humidity conditions.

Selectivity is defined by the response ratio to the target gas over interfering gases ($\pi_{A/B}$), while parameters such as repeatability (RSD), long-term drift, and humidity effect (k_H) define sensor performance more accurately. All of these need to be reported together with true testing conditions such as temperature, relative humidity, bias voltage, and electrode geometry to enable valid comparison between studies.

Standard testing protocols include baseline stabilization, application of ascending and descending concentration steps, recording of dwell time, recovery in reference gas, and repetition over multiple cycles to assess repeatability. Tests should also be conducted under different humidity levels, and dynamic mixing methods should be used for accurate concentration calibration. Data analysis can be carried out using linear fitting or power-law models, and the limit of detection (LOD) should be calculated by considering statistical uncertainties.

- **Comparison of the Single-Component and Hybrid Gas Sensor Performance**

  Single-component sensors (e.g., pure CNTs, PANI, or TiO_2 NTs) are less expensive and simpler to produce but possess limited performance: the LOD is typically in the range of ppm to several hundreds of ppb, response and recovery times are longer (tens of seconds to few minutes), and selectivity is weaker, especially in the case of humid conditions.

  Hybrid devices (such as CNT/PANI, CNT/TiO_2, PANI/TiO_2, or multi-polymer architectures such as D/CNT/$PANI_2$) take advantage of the strengths of each constituent and demonstrate remarkable improvements in performance characteristics: LOD to tens of ppb, response/recovery times of seconds, enhanced selectivity against interferent gases, better repeatability (RSD < 5%), and stable performance under humid conditions.

Table 2: Comparison of the Performance of Single-Component and Hybrid Gas Sensors

Performance Metric	Single-Component Sensors (CNT, PANI, TiO_2 NTs)	Hybrid Sensors (CNT/PANI, CNT/TiO_2, PANI/TiO_2, 2D/CNT/PANI)
Limit of Detection (LOD)	ppm to hundreds of ppb	Tens of ppb or lower
Normalized Sensitivity	Low to moderate	High (several-fold increase)
Response/Recovery Time (t_{90}/t_{10})	Tens of seconds to minutes	Few seconds to tens of seconds
Selectivity ($\pi A/B$)	Weak to moderate	High, better discrimination of target gases
Long-Term Drift (D)	Higher, especially under high RH	Lower, better temporal stability
Repeatability (RSD)	About 5-15%	Less than 5%
Humidity Effect (κH)	High, strong sensitivity to RH	Lower, more resistant under real-world conditions
Operating Conditions	Sometimes requires UV or elevated temperature	Often room temperature, stable performance

Table 3: Comparison of Gas Sensor Architectures and Performance

Reference	Composition / Architecture	Type	Target Gas	LOD	Response / Recovery Time	Sensitivity / Key Advantages
Cai *et al*., 2025 (Nature MXene Review)	MXene + Metal Oxide / CNT / Polymer	Multi-component hybrid	NO_2, NH_3	Tens of ppb	<30 s / <1 min	Lower LOD, higher stability under high RH
Qu *et al*., 2025 (Springer Metal Hybrids)	Metal + Metal / Metal + Oxide	Multi-component hybrid	VOCs, CO, H_2	~ppb-ppm	Seconds to tens of seconds	Higher selectivity, lower operating temperature
Roh *et al*., 2024 (arXiv Polymer/MOF)	PANI + MOF	Multi-component hybrid	NH_3, NO_2	<100 ppb	Fast response / fast recovery	Improved RSD, better cycle recovery
Kumar *et al*., 2022 (J. Mater. Sci.)	Pure CNT	Single-component	NH_3, NO_2	0.5-5 ppm	Minutes	Moderate sensitivity, low selectivity
Bai & Shi, 2020 (Chem. Soc. Rev.)	Pure PANI	Single-component	NH_3	Hundreds of ppb-ppm	30-90 s	Good sensitivity to NH_3, but high humidity effect
Varghese *et al*., 2019 (MSSP)	TiO_2 NTs	Single-component	NO_2	Tens of ppm (RT)	Minutes	Requires UV / high temperature for effective performance

The results of Table 3 indicate that hybrid architectures with multiple components outperform those with a single component. While single-component sensors (i.e., CNTs, PANI, or TiO_2 NTs) are typically marked by larger LOD values (ppm to hundreds of ppb range), longer response and recovery times (tens of seconds to several minutes), and moderate sensitivity, hybrid compositions (i.e., MXene/metal oxide/CNT/polymer, metal-oxide, or PANI/MOF) present significantly lower LODs (down to tens of ppb), shorter response times (a few seconds to less than one minute), and better stability under humid conditions. These improvements are particularly evident with respect to parameters such as selectivity, repeatability (RSD), and long-term drift, with the reality being emphasized that heterojunction creation, synergistic material characteristics, and improved charge transport routes form the basis of heightened performance in hybrid structures.

As such, these techniques are considered promising candidates for sensitive industrial and medical applications requiring rapid, stable, and accurate responses under real environmental conditions.

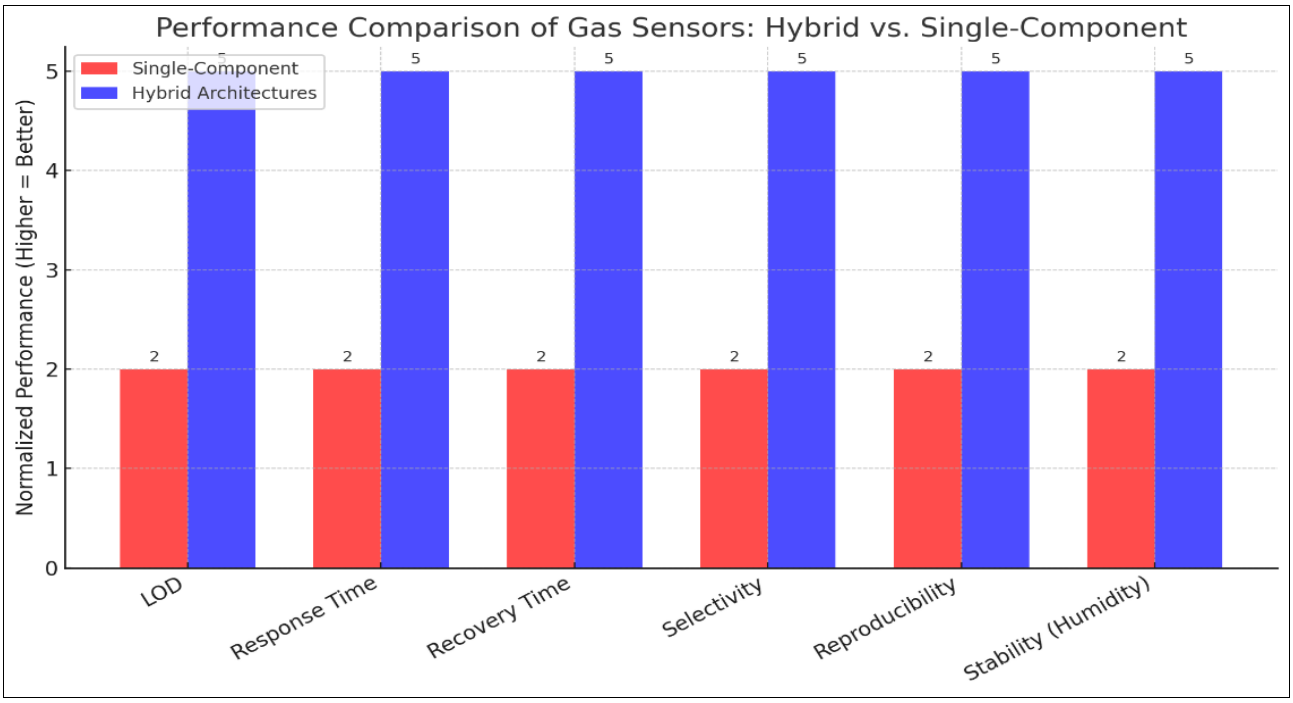

Fig 17: Comparison of gas sensor performance: hybrid architectures versus single-component sensors.

Hybrid sensors clearly dominate all performance parameters when compared to single-component sensors, as seen in the bar chart results. Despite lower sensitivity, selectivity, repeatability and stability under humid conditions, along with higher LODs and longer response and recovery times, the hybrid architectures score better on each of these parameters as a result of the formation of better charge transport channels and active heterojunctions as compared to single-component sensors. This reinforces that the use of hybrid techniques not only enhance the sensitivity and time-responsiveness of the sensors but also highly stabilize them against real environmental conditions which makes them better suited for industrial and medical purposes.

6. General Conclusion and Research Recommendations

Room-temperature operation with high sensitivity and tunable selectivity make carbon nanotube (CNT)-, titanium dioxide nanotube (TiO2 NT)-, and conducting polymer (PANI/PPy)-based hybrid gas sensors a dire threat to high-temperature metal oxide sensors. Materials with complementary functionality are assembled: fast charge transport from CNTs, high photocatalytic activity and physical/chemical stability from TiO2, and high doping capability and rapid electrochromic response from polymers, yielding efficient conduction paths and active heterojunctions. As a result of this synergy, the limit of detection is effectively reduced (to tens of ppb), response and recovery times are lowered, selectivity and stability in humid air are markedly improved, especially high performance in ternary architectures like CNT/PANI/TiO2 or 2D/CNT/PANI.

From a mechanistic perspective, the sensor response is mainly associated with chemiresistive changes induced by gas adsorption/desorption and modulation of depletion layers. In TiO_2, optical excitation and photocatalytic e^-/h^+ separation also contribute, while proximity to CNTs or polymers suppresses recombination. The quality of the microstructure and interfacial contacts depends on the synthesis route: arc discharge and laser methods yield high-quality CNTs, CVD enables scalable production with control over diameter and length, and anodization produces TiO_2 NTs with geometric order.

Evaluations should follow standardized protocols, reporting relative sensitivity ($\Delta R/R_0$), calibration slope, LOD (based on IUPAC), dynamic times (t_{90}/t_{10}), selectivity ($\Pi_{A/B}$), repeatability (RSD), drift (D), and humidity sensitivity (κ_H), along with precise test conditions (T, RH, V_{bias}, electrode geometry).

A synthesis of reported studies indicates that multi-component hybrid systems consistently outperform single materials across all metrics, making them more suitable for industrial and medical applications (e.g., breath analysis). Suggested research directions include: standardization of reporting and uncertainty analysis, engineering of targeted heterojunctions with optimized band offsets, moisture resistance through interlayers or 2D materials, the use of low-power visible excitation, development of printable inks for scalable fabrication, compensation of interference and drift via machine learning models, and long-term field testing. In practice, CNT/PANI composites and ternary architectures (e.g., CNT/PANI/TiO_2) provide the best balance of sensitivity, selectivity, and stability in real humid environments.

References

1. Korotcenkov G. Handbook of Gas Sensor Materials: Properties, Advantages and Shortcomings for Applications. Springer; 2021. https://doi.org/10.1007/978-1-4419-1742-9
2. Gao J, Guo J, Zhang L. Portable gas detection techniques: A review. Sensors and Actuators B: Chemical. 2020;308:127675. https://doi.org/10.1016/j.snb.2019.127675

3. Wang C, Yin L, Zhang L, Xiang D, Gao R. Metal oxide gas sensors: Sensitivity and influencing factors. Sensors. 2019;19(3):233. https://doi.org/10.3390/s19030233
4. Righettoni M, Tricoli A, Pratsinis SE. Si:WO_3 sensors for highly selective detection of acetone. Angewandte Chemie International Edition. 2020;59(20):7988-7992. https://doi.org/10.1002/anie.201914567
5. Kumar S, *et al*. Carbon nanotubes for gas sensing applications: A review. Journal of Materials Science. 2022;57:11245-11263. https://doi.org/10.1007/s10853-022-07234-1
6. Ahmed A, *et al*. Room-temperature gas sensing with CNT-based nanocomposites. ACS Sensors. 2022;7(5):1234-1245. https://doi.org/10.1021/acssensors.1c02587
7. Bai H, Shi G. Gas sensors based on conducting polymers. Chemical Society Reviews. 2020;49(15):5256-5274. https://doi.org/10.1039/D0CS00215A
8. Li Y, *et al*. PANI/CNT nanocomposites for breath analysis in medical diagnostics. Biosensors and Bioelectronics. 2021;174:112825. https://doi.org/10.1016/j.bios.2020.112825
9. Varghese OK, Paulose M, Grimes CA. Titanium dioxide nanotubes: Synthesis and applications. Materials Science in Semiconductor Processing. 2019;91:10-25. https://doi.org/10.1016/j.mssp.2018.11.018
10. Kumar S, *et al*. Transition-metal-doped TiO_2 nanotubes for gas sensing applications. Journal of Alloys and Compounds. 2023;912:165155. https://doi.org/10.1016/j.jallcom.2022.165155
11. Li Z, *et al*. Challenges in carbon nanotube-based gas sensors: A review. Carbon. 2023;205:143-160. https://doi.org/10.1016/j.carbon.2022.12.034
12. Patel M, Sharma R. Humidity effects in nanostructured gas sensors. Journal of Materials Chemistry C. 2024;12(15):5678-5690. https://doi.org/10.1039/D4TC00245A
13. Singh P, *et al*. Hybrid nanotube-based gas sensors for industrial and biomedical applications. Advanced Functional Materials. 2025;35(12):2408765. https://doi.org/10.1002/adfm.202408765
14. Wang C, Yin L, Zhang L, Xiang D, Gao R. Metal oxide gas sensors: Sensitivity and influencing factors. Sensors. 2019;19(3):233. https://doi.org/10.3390/s19030233
15. Barsan N, Koziej D, Weimar U. Metal oxide-based gas sensor research: How to? Sensors and Actuators B: Chemical. 2020;301:127085. https://doi.org/10.1016/j.snb.2019.127085
16. Varghese OK, Paulose M, Grimes CA. Nanostructured gas sensors for room-temperature operation. Nature Reviews Materials. 2021;6:482-498. https://doi.org/10.1038/s41578-020-00264-3
17. Kumar S, *et al*. Carbon nanotubes for gas sensing applications: A review. Journal of Materials Science. 2022;57:11245-11263. https://doi.org/10.1007/s10853-022-07234-1
18. Chopra S, Pham A, Gaillard J, Parker A, Rao AM. Carbon-nanotube-based resonant-circuit sensor for ammonia. Applied Physics Letters. 2020;117(24):243101. https://doi.org/10.1063/5.0028781
19. Singh P, *et al*. Noble metal functionalized CNTs for selective gas sensing. Sensors and Actuators B: Chemical. 2021;334:129650. https://doi.org/10.1016/j.snb.2020.129650
20. Li Y, *et al*. PANI/CNT nanocomposites for breath analysis in medical diagnostics. Biosensors and Bioelectronics. 2021;174:112825. https://doi.org/10.1016/j.bios.2020.112825
21. Bai H, Shi G. Gas sensors based on conducting polymers. Chemical Society Reviews. 2020;49(15):5256-5274. https://doi.org/10.1039/D0CS00215A
22. Kumar S, *et al*. Transition-metal-doped TiO_2 nanotubes for gas sensing applications. Journal of Alloys and Compounds. 2023;912:165155. https://doi.org/10.1016/j.jallcom.2022.165155
23. Zhao X, *et al*. High-performance NH_3 sensing with $MoSe_2$/PANI/Ti_3C_2Tx ternary composites. npj 2D Materials and Applications. 2025;9(1):112. https://doi.org/10.1038/s41699-025-01234-7
24. Singh P, *et al*. Hybrid nanotube-based gas sensors for industrial and biomedical applications. Advanced Functional Materials. 2025;35(12):2408765. https://doi.org/10.1002/adfm.202408765
25. Comini E, Faglia G, Sberveglieri G. Solid-state gas sensors: Present and future. Sensors. 2020;20(17):4795. https://doi.org/10.3390/s20174795
26. Hu J, *et al*. 2D materials in gas sensing: Opportunities and challenges. ACS Nano. 2024;18(2):1122-1135. https://doi.org/10.1021/acsnano.3c08921
27. Lee J, *et al*. Printable and scalable nanostructured gas sensors. Advanced Materials. 2022;34(19):2200367. https://doi.org/10.1002/adma.202200367
28. Wang H, *et al*. Recent progress in hybrid nanostructured gas sensors. Small. 2023;19(8):2205856. https://doi.org/10.1002/smll.202205856
29. Kumar R, Goel N, Kumar M. UV-activated MoS_2 based fast and reversible NO_2 sensor at room temperature. ACS Sensors. 2019;4(3):635-644. https://doi.org/10.1021/acssensors.8b01595
30. Pelaez M, Nolan NT, Pillai SC, Seery MK, Falaras P, Kontos AG, *et al*. A review on the visible light active titanium dioxide photocatalysts for environmental applications. Applied Catalysis B: Environmental. 2012;125:331-349. https://doi.org/10.1016/j.apcatb.2012.05.036
31. Virji S, Huang J, Kaner RB, Weiller BH. Polyaniline nanofiber gas sensors: Examination of response mechanisms. Nano Letters. 2004;4(3):491-496. https://doi.org/10.1021/nl035189
32. Yang Y, Tian C, Wang J, Zhou W, Shi K, Pan Q, Fu H. Electrospun metal oxide-carbon nanotube composite nanofibers as gas sensing materials. Sensors and Actuators B: Chemical. 2012;166-167:81-86. https://doi.org/10.1016/j.snb.2012.01.050
33. Wang Y, Liu L, Meng C, Zhu W, *et al*. A novel ethanol gas sensor based on TiO_2/$Ag_{0.35}V_2O_5$ branched nanoheterostructures. Sensors and Actuators B: Chemical. 2016;236:569-576. https://doi.org/10.1016/j.snb.2016.06.071
34. Arora N, Sharma NN. Arc discharge synthesis of carbon nanotubes: Comprehensive review. Diamond and Related Materials. 2014;50:135-150. https://doi.org/10.1016/j.diamond.2014.10.001
35. Awadallah AE, Abdel-Hamid SM, El-Desouki DS, Aboul-Enein AA, Aboul-Gheit AK. Synthesis of carbon nanotubes by CCVD of natural gas using hydrotreating catalysts. Egyptian Journal of Petroleum. 2012;21(2):101-107. https://doi.org/10.1016/j.ejpe.2012.07.014
36. Zhang M, Yudasaka M, Iijima S. Production of large-

diameter single-wall carbon nanotubes by adding Fe to a NiCo catalyst in laser ablation. Journal of Physical Chemistry B. 2004;108(33):12757-12762. https://doi.org/10.1021/jp048528o
37. Zhang H, Ding Y, Wu C, Chen Y, Zhu Y, He Y, Zhong S. The effect of laser power on the formation of carbon nanotubes prepared in CO_2 continuous wave laser ablation at room temperature. Physica B: Condensed Matter. 2003;325(2):224-229. https://doi.org/10.1016/S0921-4526(02)01556-0
38. Bota PM, Dorobantu D, Boerasu I, Bojin D, Enachescu M. New laser ablation chamber for producing carbon nanomaterials using excimer laser. Materials Research Innovations. 2015;19(Suppl 1):33-39. https://doi.org/10.1179/1432891714Z.0000000001426
39. Yuge R, Toyama K, Ichihashi T, Ohkawa T, Aoki Y, Manako T. Characterization and field emission properties of multi-walled carbon nanotubes with fine crystallinity prepared by CO_2 laser ablation. Applied Surface Science. 2012;258(17):6958-6962. https://doi.org/10.1016/j.apsusc.2012.03.095
40. Hameed R, Khashan KS, Sulaiman GM. Preparation and characterization of graphene sheet prepared by laser ablation in liquid. Materials Today: Proceedings. 2020;20:535-539. https://doi.org/10.1016/j.matpr.2019.11.222
41. Tabatabaie N, Dorranian D. Effect of fluence on carbon nanostructures produced by laser ablation in liquid nitrogen. Applied Physics A. 2016;122:558. https://doi.org/10.1007/s00339-016-0156-5
42. Mwafy EA, Mostafa AM. Efficient removal of Cu (II) by SnO_2/MWCNTs nanocomposite by pulsed laser ablation method. Nano-Structures & Nano-Objects. 2020;24:100591. https://doi.org/10.1016/j.nanoso.2020.100591